

Crossover of the dynamical behavior in two-dimensional random transverse Ising model

Shu-Xia Chen, Yin-Yang Shen, and Xiang-Mu Kong*

Shandong Provincial Key Laboratory of Laser Polarization and Information Technology, Department of Physics, Qufu Normal University, Qufu 273165, China

(Received 12 December 2009; revised manuscript received 1 October 2010; published 3 November 2010)

The dynamics of the two-dimensional spin- $\frac{1}{2}$ random transverse Ising model is studied by means of the recurrence relations method. Both the autocorrelation functions and the corresponding spectral densities are calculated in the cases that the exchange couplings or fields satisfy three typical distributions, respectively. For the cases of Gaussian and double-Gaussian distribution, when the standard deviation of the random variable is small, the dynamics of the system undergoes a crossover from a central-peak behavior to a collective-mode one, the result is similar to that of the bimodal distribution. While the standard deviation is large enough, the crossover disappears and the dynamics of the system shows a central-peak behavior or a disordered behavior.

DOI: [10.1103/PhysRevB.82.174404](https://doi.org/10.1103/PhysRevB.82.174404)

PACS number(s): 75.40.Gb, 75.10.Jm, 75.50.Lk

I. INTRODUCTION

The dynamical behavior of quantum spin systems has attracted a great deal of attention in both theory and experiment in the past decades.¹ In particular, the transverse Ising model (TIM) and the XY model have attracted considerable interest.² It is well known that the time-dependent correlation function plays an important role in the study of the dynamical properties of many-body systems. For one-dimensional (1D) pure spin systems, the time-dependent correlation function (e.g., autocorrelation function) has been calculated exactly,³⁻⁸ and it exhibits a Gaussian decay in the infinite temperature limit,^{6,7} a power-law decay at zero temperature,^{3,4} and an exponential behavior at $0 < T < \infty$ (T is the temperature of the system).⁸ Besides, Niemeijer calculated the longitudinal correlation function exactly in the high-temperature limit for the isotropic XY chain, and obtained the function $C(t) = \langle S_i^z(t) S_i^z(0) \rangle = J_0(2Jt)^2/4$, where S_i^z are spin operators, J_0 is the zeroth order Bessel function, and J is the nearest-neighbor exchange coupling energy.⁹ In the low temperature case, $C(t)$ of the 1D isotropic XY system were obtained by Katsura with the two-time Green's-function method.¹⁰

Recently, the random quantum spin systems, in which the exchange couplings J_i or the external fields B_i are random variables, such as the 1D random transverse Ising model, XY model, and Heisenberg model, have been paid considerable attention.¹¹⁻¹⁷ Florencio and Barreto studied the 1D random TIM (RTIM) with bimodal distribution and found that the dynamical behavior of the system undergoes a crossover from a central-peak behavior onto a collective-mode behavior.¹¹ Then, this model with four-spin interactions was investigated by Boechat, and it is shown that disorder induces a crossover mentioned above as the concentration of weaker bonds (or bond dilution) is enhanced.¹² For the 1D random XY model, Nunes found that the long-time dynamical behavior is governed by the stronger couplings.¹³ Nunes also investigated both the XY chain and XY ladder with Ising interchain couplings in the presence of random fields, and it is found that the dynamics is sensitive to the percentage of disorder but not to the intensity of the field.¹⁴ Recently, we studied the effects of Gaussian distribution on

the dynamics of 1D RTIM and found that this system exhibits two crossovers when the standard deviation of random exchange coupling or random external field is small, however, there is no crossover when the standard deviation is large enough.¹⁵ We also investigated the 1D random transverse XY model with double-Gaussian distribution and found that the system undergoes a crossover.¹⁶ Considering nearest-neighbor and next-nearest-neighbor interactions, the central-peak behavior becomes more obvious and the collective-mode behavior becomes weaker in the 1D RTIM.¹⁷

All the systems above are one-dimensional. It is well known, the two-dimensional (2D) quantum spin systems are quite interesting from the viewpoint of theoretical research and practical application. However, solving the 2D Ising model exactly is very difficult.¹⁸ Although some works were made aiming at the dynamics of the 2D pure transverse Ising model¹⁹ in the high-temperature limit or zero-temperature dynamics of the 2D Ising model with zero magnetic field,²⁰ no unambiguous interpretation has been given on the 2D RTIM. In this work, we shall focus on the time evolution of this system in the high-temperature limit. Our main purpose is to calculate both the autocorrelation function and the corresponding spectral densities in the presence of disorder. We are also interested in the effects of the different disorder on the dynamics.

This paper is organized as follows: in Sec. II, we introduce the 2D RTIM and study the effects of bimodal disorder on the dynamics. The results and discussions for the Gaussian disorder and the double-Gaussian disorder are given in Secs. III and IV, respectively. Section V is the conclusion.

II. DYNAMICS OF THE BIMODAL DISTRIBUTION

Consider the two-dimensional Ising model on a square lattice with n rows and n columns, and it is in an external magnetic field along the z axis. The Hamiltonian of such system can be described by

$$H = -\frac{1}{2} \sum_{i=1}^n \sum_{j=1}^n (J_{ij,ij+1} \sigma_{i,j}^x \sigma_{i,j+1}^x + J_{ij,i+1,j} \sigma_{i,j}^x \sigma_{i+1,j}^x) - \frac{1}{2} \sum_{i=1}^n \sum_{j=1}^n B_{i,j} \sigma_{i,j}^z, \quad (1)$$

where $\sigma_{i,j}^\alpha (\alpha=x, y, z)$ is the Pauli matrix at site (i, j) , which is the site of the i th row and the j th column on the square lattice. $J_{ij,i'j'}$ and $B_{i,j}$ are nearest-neighbor exchange couplings and the transverse fields, respectively. In this work, we consider the magnetic fields and the exchange couplings as random variables.

It is well known that the dynamics of the 2D RTIM can be studied by calculating the average spin autocorrelation function which can be defined as

$$C(t) = \overline{\langle \sigma_{i,j}^x(0) \sigma_{i,j}^x(t) \rangle}, \quad (2)$$

where $\overline{\langle \dots \rangle}$ denotes an ensemble average followed by an average over the random variable. We are also interested in the spectral density $\Phi(\omega)$ which is defined as the Fourier transformation of the spin-correlation function,

$$\Phi(\omega) = \int_{-\infty}^{+\infty} e^{i\omega t} C(t) dt. \quad (3)$$

It is useful to understand the dynamics of the system since different dynamic behaviors exhibit distinct signatures depend on $\Phi(\omega)$. The spectral density can be also measured directly by neutron-scattering experiment.

In order to calculate the spin autocorrelation function $C(t)$ and the spectral density $\Phi(\omega)$, we use the method of recurrence relations which has been applied to a lot of dynamical problems.^{11,15,21-23} Base on this method, $C(t)$ is written as the form of moment expansion

$$C(t) = \sum_{k=0}^{\infty} \frac{(-1)^k}{(2k)!} \mu^{2k} t^{2k} \quad (4)$$

with

$$f_1 = B_{i,j} \sigma_{i,j}^y,$$

$$f_2 = (\Delta_1 - B_{i,j}^2) \sigma_{i,j}^x + B_{i,j} J_{i-1,j} \sigma_{i-1,j}^x \sigma_{i,j}^z + B_{i,j} J_{i,j-1} \sigma_{i,j-1}^x \sigma_{i,j}^z + B_{i,j} J_{i,j} \sigma_{i,j+1}^x \sigma_{i,j}^z + B_{i,j} J_{i,j} \sigma_{i+1,j}^x \sigma_{i,j}^z,$$

$$f_3 = -B_{i,j} (-\Delta_1 - \Delta_2 + B_{i,j}^2 + J_{i,j-1}^2 + J_{i-1,j}^2 + 2J_{i,j}^2) \sigma_{i,j}^y - 2B_{i,j} J_{i,j-1} J_{i-1,j} \sigma_{i-1,j}^x \sigma_{i,j-1}^x \sigma_{i,j}^y - 2B_{i,j} J_{i,j} J_{i-1,j} \sigma_{i-1,j}^x \sigma_{i,j+1}^x \sigma_{i,j}^y - 2B_{i,j} J_{i,j-1} J_{i,j} \sigma_{i,j-1}^x \sigma_{i+1,j}^x \sigma_{i,j}^y - 2B_{i,j} J_{i,j-1} J_{i,j} \sigma_{i,j-1}^x \sigma_{i+1,j}^x \sigma_{i,j}^y - 2B_{i,j} J_{i,j}^2 \sigma_{i,j+1}^x \sigma_{i+1,j}^x \sigma_{i,j}^y + B_{i-1,j} B_{i,j} J_{i-1,j} \sigma_{i-1,j}^y \sigma_{i,j}^z + B_{i,j-1} B_{i,j} J_{i,j-1} \sigma_{i,j-1}^y \sigma_{i,j}^z + B_{i,j} B_{i,j+1} J_{i,j} \sigma_{i,j+1}^y \sigma_{i,j}^z + B_{i,j} B_{i+1,j} J_{i,j} \sigma_{i+1,j}^y \sigma_{i,j}^z.$$

The inner products of the basis vectors are acquired as follows:

$$\mu^{2k} = \frac{1}{Z} \text{Tr} \sigma_{i,j}^x \{H, [H, \dots (H, \sigma_{i,j}^x), \dots]\}, \quad (5)$$

where μ^{2k} is the $2k$ th moment of $C(t)$. Supposing that the first 18th moments have been calculated by Eq. (5), we can calculate the spin autocorrelation function by means of constructing the Padé approximant. In order to calculate $\Phi(\omega)$, we consider the time-dependent spin $\sigma_{i,j}^x(t)$ which is expanded in a d -dimensional Hilbert space S ,

$$\sigma_{i,j}^x(t) = \sum_{\nu=0}^{d-1} a_\nu(t) f_\nu, \quad (6)$$

where $a_\nu(t)$ are time-dependent real functions and f_ν are basic vectors spanning S . Set the zeroth basis vector $f_0 = \sigma_{i,j}^x(0)$, the remaining f_ν satisfy the recurrence relation (RRI)

$$f_{\nu+1} = iL f_\nu + \Delta_\nu f_{\nu-1}, \quad 0 \leq \nu \leq d-1, \quad (7)$$

where $L f_\nu = [H, f_\nu] = H f_\nu - f_\nu H$, and the continued-fraction coefficients $\Delta_\nu = \frac{(f_\nu, f_\nu)}{(f_\nu, f_{\nu-1})}$, with $\Delta_0 = 1$ and $f_{-1} = 0$, where $(f_\nu, f_\nu) = \langle f_\nu | f_\nu \rangle$ is the inner product of the basis vectors.

The $a_\nu(t)$'s satisfy the second recurrence relation

$$\Delta_{\nu+1} a_{\nu+1}(t) = -\frac{da_\nu(t)}{dt} + a_{\nu-1}(t), \quad \nu \geq 0 \quad (8)$$

with $a_{-1}(t) \equiv 0$. Using $a_0(z) = \int_0^\infty e^{-zt} a_0(t) dt$, where $a_0(t) = C(t)$, $z = \varepsilon + i\omega$, $\varepsilon > 0$, we can obtain the continued fraction

$$a_0(z) = \frac{1}{z + \frac{\Delta_1}{z + \frac{\Delta_2}{z + \dots}}}, \quad (9)$$

which can be useful to calculate the spectral density, i.e.,

$$\Phi(\omega) = \lim_{\varepsilon \rightarrow 0} \text{Re} a_0(z).$$

We have obtained the first eight basis vectors. For the reason that the basis vectors become very length with the increasing of ν , we just show the simple ones of them,

$$(f_0, f_0) = 1,$$

$$(f_1, f_1) = \overline{B_{i,j}},$$

$$(f_2, f_2) = \overline{\Delta_1^2} - 2\overline{\Delta_1 B_{i,j}^2} + \overline{B_{i,j}^4} + \overline{B_{i,j}^2 J_{i-1,j}^2} + \overline{B_{i,j}^2 J_{i,j-1}^2} + 2\overline{B_{i,j}^2 J_{i,j}^2},$$

$$\begin{aligned} (f_3, f_3) = & \overline{B_{i-1,j}^2 B_{i,j}^2 J_{i-1,j}^2} + \overline{B_{i,j-1}^2 B_{i,j}^2 J_{i,j-1}^2} + 4\overline{\Delta_1^2 B_{i,j}^4 J_{i-1,j}^2 J_{i,j-1}^2} + 8\overline{\Delta_1 \Delta_2 B_{i,j}^4 J_{i-1,j}^2 J_{i,j-1}^2} + 4\overline{\Delta_2^2 B_{i,j}^4 J_{i-1,j}^2 J_{i,j-1}^2} - 8\overline{\Delta_1 B_{i,j}^6 J_{i-1,j}^2 J_{i,j-1}^2} \\ & - 8\overline{\Delta_2 B_{i,j}^6 J_{i-1,j}^2 J_{i,j-1}^2} + 4\overline{B_{i,j}^8 J_{i-1,j}^2 J_{i,j-1}^2} - 8\overline{\Delta_1 B_{i,j}^4 J_{i-1,j}^4 J_{i,j-1}^2} - 8\overline{\Delta_2 B_{i,j}^4 J_{i-1,j}^4 J_{i,j-1}^2} + 8\overline{B_{i,j}^6 J_{i-1,j}^4 J_{i,j-1}^2} + 4\overline{B_{i,j}^4 J_{i-1,j}^6 J_{i,j-1}^2} \\ & - 8\overline{\Delta_1 B_{i,j}^4 J_{i-1,j}^2 J_{i,j-1}^4} - 8\overline{\Delta_2 B_{i,j}^4 J_{i-1,j}^2 J_{i,j-1}^4} + 8\overline{B_{i,j}^6 J_{i-1,j}^2 J_{i,j-1}^4} + 8\overline{B_{i,j}^4 J_{i-1,j}^4 J_{i,j-1}^2} + 4\overline{B_{i,j}^4 J_{i-1,j}^2 J_{i,j-1}^6} + \overline{B_{i,j}^2 B_{i+1,j}^2 J_{i,j}^2} \\ & + \overline{B_{i,j}^2 B_{i+1,j}^2 J_{i,j}^2} \\ & + 8\overline{B_{i,j}^2 J_{i-1,j}^2 J_{i,j}^2} + 8\overline{B_{i,j}^2 J_{i,j-1}^2 J_{i,j}^2} - 16\overline{\Delta_1 B_{i,j}^4 J_{i-1,j}^2 J_{i,j-1}^2 J_{i,j}^2} - 16\overline{\Delta_2 B_{i,j}^4 J_{i-1,j}^2 J_{i,j-1}^2 J_{i,j}^2} + 16\overline{B_{i,j}^6 J_{i-1,j}^2 J_{i,j-1}^2 J_{i,j}^2} + 16\overline{B_{i,j}^4 J_{i-1,j}^2 J_{i,j-1}^2 J_{i,j}^2} \\ & + 16\overline{B_{i,j}^4 J_{i-1,j}^2 J_{i,j-1}^2 J_{i,j}^4} + 4\overline{B_{i,j}^4 J_{i,j}^4} + 16\overline{B_{i,j}^4 J_{i-1,j}^2 J_{i,j-1}^2 J_{i,j}^4}. \end{aligned}$$

Then, the first seven continued-fraction coefficients can be obtained. However, because of the mathematical complexity, only a finite number of Δ_p can be calculated. Thus it is necessary to truncate $a_0(z)$ by introducing a terminating function-Gaussian terminator.^{24,25}

In this section, assume that the exchange couplings $J_{ij,i'j'}$ and the transverse fields $B_{i,j}$ are independent variables drawn from the bimodal distribution

$$\rho(J_{ij,i'j'}) = p\delta(J_{ij,i'j'} - J_1) + (1-p)\delta(J_{ij,i'j'} - J_2), \quad (10)$$

$$\rho(B_{i,j}) = q\delta(B_{i,j} - B_1) + (1-q)\delta(B_{i,j} - B_2), \quad (11)$$

respectively, where p (q) represents the probability of the exchange coupling J_1 (the field B_1), and $1-p$ ($1-q$) represents the probability of J_2 (B_2), $0 \leq p \leq 1$.

Firstly, we consider the case that the exchange couplings satisfy the bimodal distribution, Eq. (10), while the external fields are uniform, $B_{i,j} = B = 1$, and set $J_1 = 1.0$ and $J_2 = 0.4$. In this case, we can get nine basis vectors in the front. The first nine recurrants for several values of p are shown in Fig. 1. Then the numerical results of the spin autocorrelation function $C(t)$ and corresponding spectral densities $\Phi(\omega)$ are calculated and shown in Fig. 2.

From Fig. 2, we can see that there are two types of dynamic behavior which changed with different values of p : the collective-mode behavior and central-peak behavior. When $p=0$ or 0.25, $C(t)$ shows an oscillatory behavior which is typical of collective mode while the exchange coupling is weaker than the transverse field, in this case the system is dominated by the transverse field. The cases $p=0.5$ and 0.75 show the appearance of the central-peak behavior and strong suppression of the collective-mode-type dynamics. As p increases further, the central-peak behavior becomes more obvious, and at $p=1$, $C(t)$ shows monotonically decreasing because the spin interactions are stronger than the fields and the system is dominated by the exchange coupling. The corresponding frequency of the maximum magnitude in $\Phi(\omega)$ changes from $\omega=1$ onto $\omega=0$. It is obvious that there is a crossover from collective-mode behavior onto the central-peak one as p increases.

Consider now the other case that the transverse fields $B_{i,j}$ satisfy the bimodal distribution, and the exchange couplings are constants ($J_{ij,i'j'} = J = 1.0$). In this distribution let the values $B_1 = 0.6$ ($q=1$) and $B_2 = 1.6$ ($q=0$), we can get the spin autocorrelation functions and the spectral densities which are plotted in Fig. 3. In that case of $q=0$, the autocorrelation function displays an oscillatory behavior and the center frequency of $\Phi(\omega)$ approaches 1. $C(t)$ shows a decay of the collective mode excitation when $q=0.25$. For the $q=0.75$ and 1.0 cases, $C(t)$ decay monotonically and the corresponding frequencies of the maximum magnitude of $\Phi(\omega)$ are at $\omega=0$, the collective-mode-type dynamics is replaced by a central-peak behavior. However, in the disordered case such as $q=0.5$, the dynamics of the system cannot be singly described by either behavior. We can observe that there is a crossover from a collective-mode behavior ($q=0, B_2 > J$) to a central-peak behavior ($q=1, B_1 < J$).

In a word, the system undergoes a crossover from central-peak behavior to a collective-mode behavior as J/B decrease. When the transverse field B is large ($B > J$), the system behaves like free spins precessing about the external field. The faint exchange coupling causes a damping of the

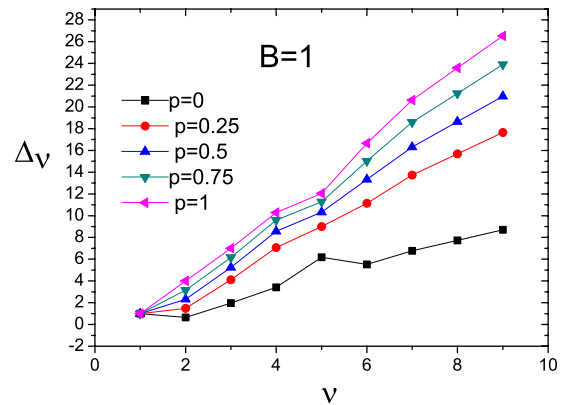


FIG. 1. (Color online) Recurrants for the random Ising model in two dimensions: the exchange couplings $J_{ij,i'j'}$ satisfy the bimodal distribution in which $J_1 = 1$ and $J_2 = 0.4$ with the probability p and $(1-p)$, respectively. The transverse fields $B_{i,j} = B = 1$.

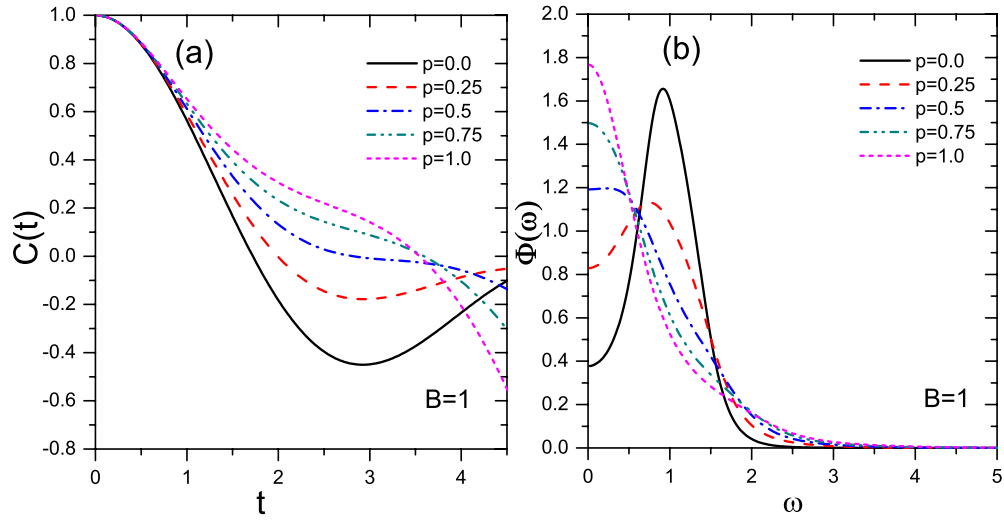


FIG. 2. (Color online) Autocorrelation functions and the spectral densities for the same parameters in Fig. 1. The system undergoes a crossover from collective-mode behavior to a central-peak one as the probability p varies from 0 ($J_{ij,i'j'} < B$) to 1 ($J_{ij,i'j'} > B$).

precessing spins and the dynamics exhibits collective-mode behavior. While $B < J$, the system is dominated by the spin-spin interactions, therefore the collective-mode disappears, and the system exhibits a central-peak behavior. The regions where the effects of disorder are being considered in the phase diagram of the pure 2D TIM in Fig. 4. The dashed line corresponds to the critical transverse field of the classical 2D Ising model for the phase transition between the ferromagnetic (Ferro) and the paramagnetic (Para) in the low-temperature region.²⁷ The dotted line ($kT_C/J=2.27$) corresponds to the critical temperature of the classical 2D Ising model.¹⁸ The open circle ($B_C/J=3.046$) corresponds to the quantum critical point of the pure system.²⁶ In the high-temperature ($T > T_C$) region, the dynamics of the system is dominated by the competition between the spin-spin interaction J and the external field B . From the result of the present system, we can see that the dynamical behavior is similar to that of the 1D RTIM studied by Florencio and Barreto.¹¹ The behavior can be understood from Ref. 7 that the Hilbert

space of σ_j^x for the 1D TIM and $\sigma_{i,j}^x$ for the 2D TIM have the same geometric structure. Besides, in the high-temperature limit, the system is in paramagnetic phase, the dynamical behavior will not be affected by phase transitions.

III. GAUSSIAN DISTRIBUTION

In the following, we consider the case in which the exchange couplings or the transverse fields satisfy the Gaussian distribution

$$\rho(\beta_{i,j}) = \frac{1}{\sqrt{2\pi}\sigma_\beta} \exp\left[-\frac{(\beta_{i,j} - \beta)^2}{2\sigma_\beta^2}\right], \quad (12)$$

where β and σ_β are the mean value and the standard deviation of $\beta_{i,j}$, respectively.

For the case that the exchange couplings $J_{ij,i'j'}$ satisfy Eq. (12) whereas the transverse fields $B_{i,j}$ remain unaltered ($B_{i,j} = B=1$). Without loss of generality, taking the mean value of

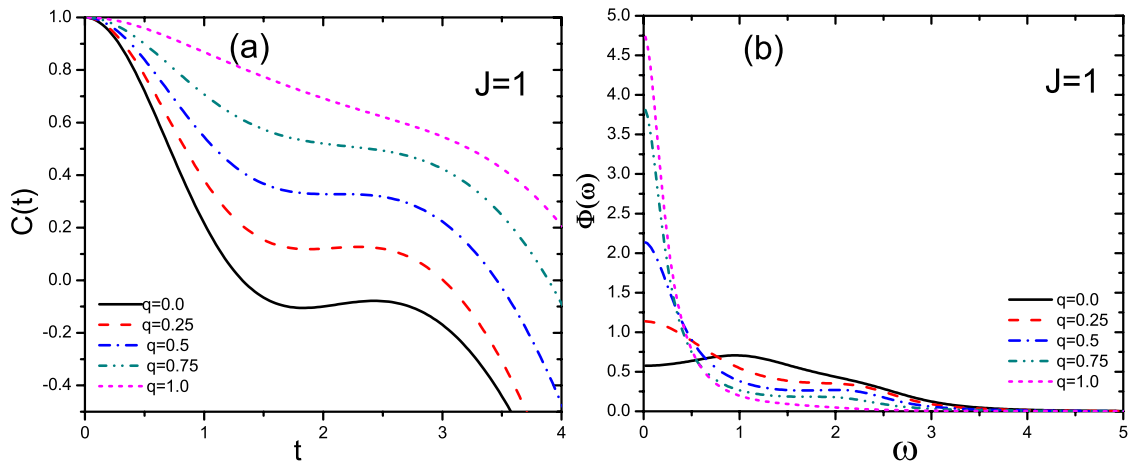


FIG. 3. (Color online) Autocorrelation functions and spectral densities for the case that the random fields satisfy the bimodal distribution while $J_{ij,i'j'}=1$. The system in a random fields $B_{i,j}$, which can take the values of 0.6 and 1.6 with the probabilities q and $1-q$. The system exhibits a crossover as q is raised from 0 to 1.

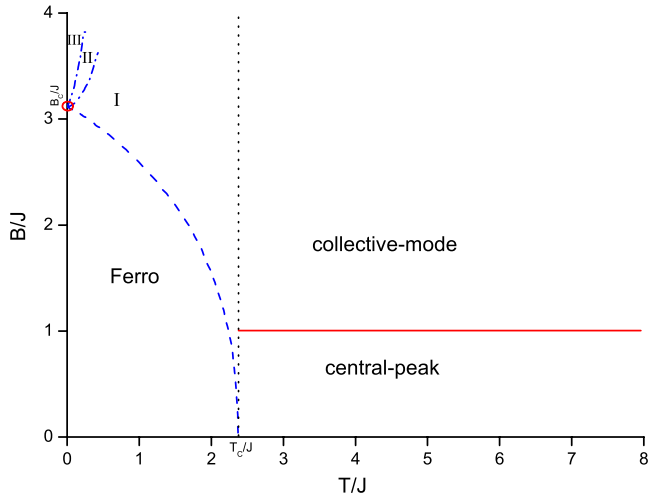


FIG. 4. (Color online) Phase diagram ($T/J, B/J$) of the pure 2D TIM. The dashed line corresponds to the critical transverse field of the classical 2D Ising model for the phase transition between the ferromagnetic (Ferro) and the paramagnetic (Para) in the low-temperature region. The regions I, II, and III correspond to three-dimensional, crossover and two-dimensional Ising behavior, respectively (Ref. 27). The dotted line ($kT_C/J=2.27$) corresponds to the critical temperature (Ref. 18) and the open circle corresponds to the quantum critical point (Ref. 26). In the high-temperature region ($T > T_C$), the system exhibits the central-peak behavior and the collective-mode one when $B/J < 1$ and $B/J > 1$, respectively. However, when $B/J \gg 1$, the system shows a disorder behavior.

the exchange couplings $J=0, 0.5, 1.0, 1.5$, and 2 , and the standard deviation $\sigma_J=0.3, 1.0, 2.0$, and 3.0 , respectively, $C(t)$ and $\Phi(\omega)$ are calculated by the recurrence relations method and the numerical results are shown in Figs. 5 and 6, respectively. The insets of Fig. 6 present the first nine continued-fraction coefficients Δ_ν ($\nu=1, 2, \dots, 9$).

Figure 5(a) shows that when the value of σ_J is small (e.g., $\sigma_J=0.3$), there are two types of dynamics: the collective-mode behavior and the central-peak behavior. When $J=0$, $C(t)$ is a slightly damped cosine function. In this case, the system behaves as independent free spins precessing about the external field. In the case of $J=0.5$, the system exhibits collective mode. Such behavior becomes weaker as the mean value J increases further. When $J=2$, the dynamics shows a central-peak behavior. In addition, the collective-mode behavior becomes weaker as the standard deviation σ_J increases [see Figs. 5(b) and 5(c)]. When σ_J is large enough (e.g., $\sigma_J=3.0$) [see Fig. 5(d)], the dynamics of the system is dominated by the spin-spin interactions and shows a central-peak behavior. The corresponding spectral densities in Fig. 6 make these different dynamics becoming more evident.

Next, consider another case in which the transverse fields $B_{i,j}$ satisfy the Gaussian distribution while the exchange couplings remain uniform ($J_{ij,i'j'}=J=1$). Let the mean value B take $0, 0.5, 1.0, 1.5$, and 2 , and the standard deviations σ_B take 0.3 and 3.0 , respectively. The numerical results of $C(t)$ and $\Phi(\omega)$ are plotted in Fig. 7. When $\sigma_B=0.3$, we can see that there is a crossover as the mean value B increases [see Fig. 7, (a1) and (a2)]. When $\sigma_B=3.0$, the crossover vanishes.

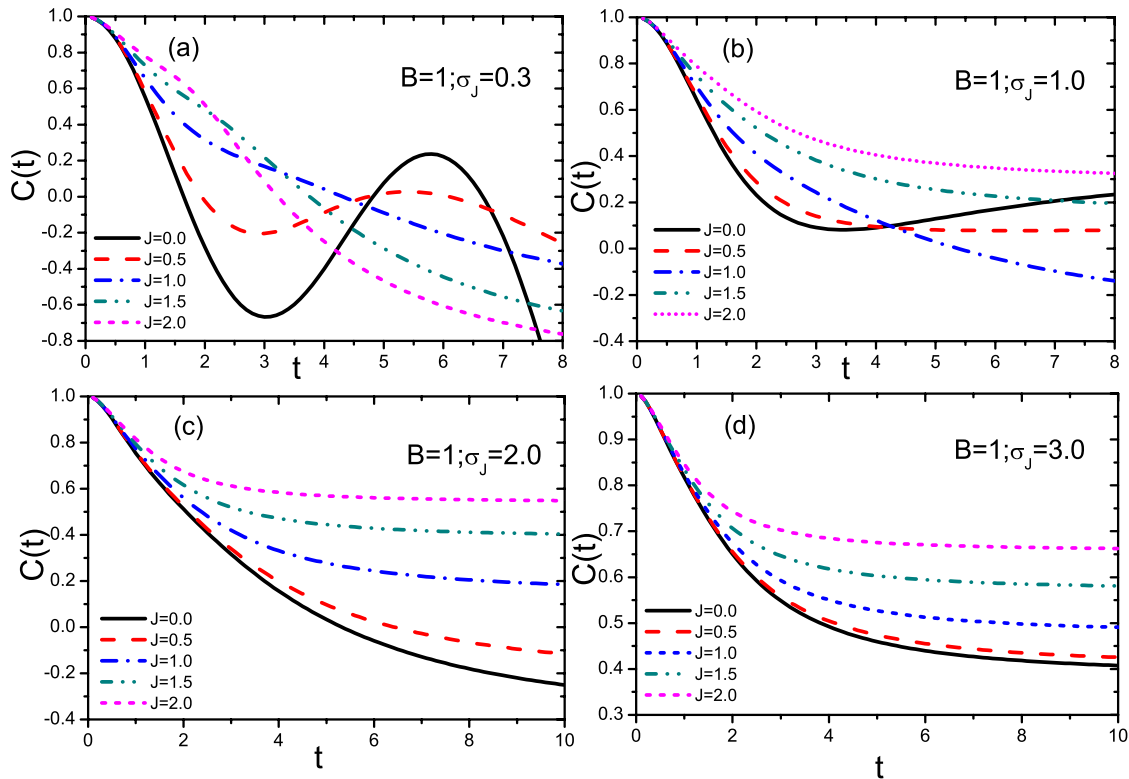


FIG. 5. (Color online) Spin autocorrelation functions for the case that the exchange couplings satisfy the Gaussian distribution and the fields are constant. The main plot shows $C(t)$ vs t for several different values of J . $\sigma_J=0.3, 1.0, 2.0, 3.0$ for the curves depicted in (a), (b), (c), and (d), respectively.

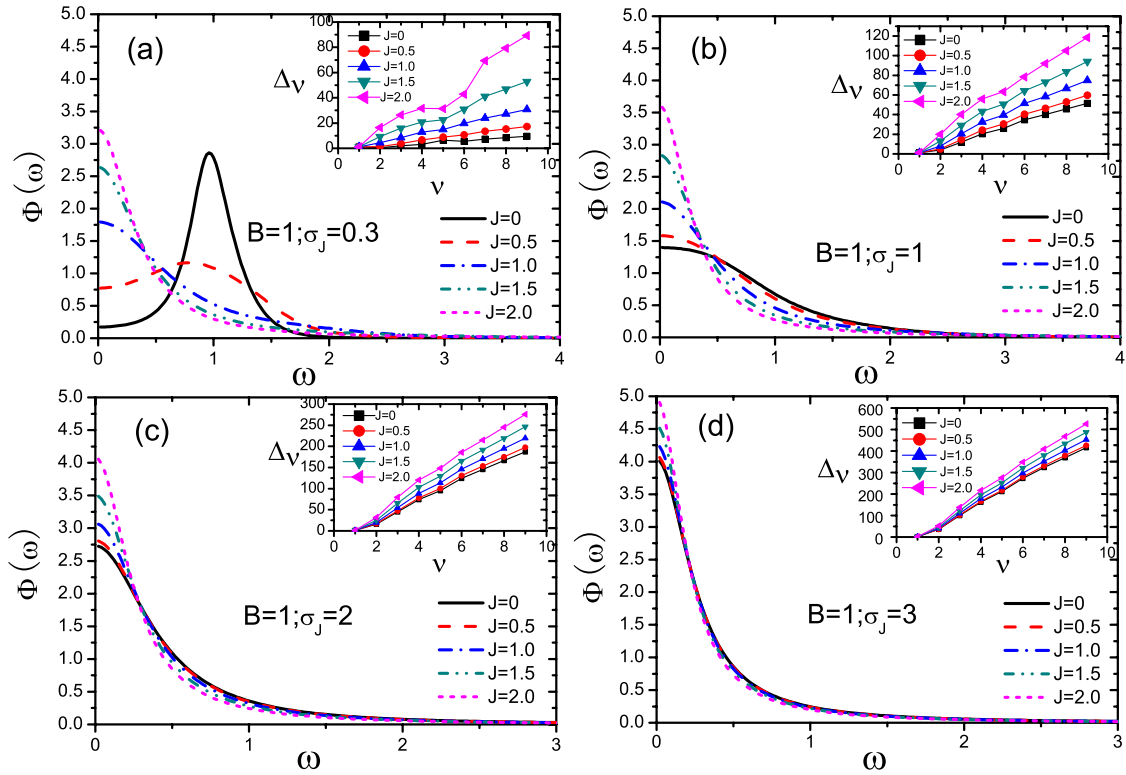


FIG. 6. (Color online) The corresponding spectral densities for the same parameters as in Fig. 5. The insets present the recurrent $\Delta_\nu(\nu=1, \dots, 9)$. As σ_J increases, the recurrants fall on a straight line. The crossover vanishes as the standard deviation increases gradually.

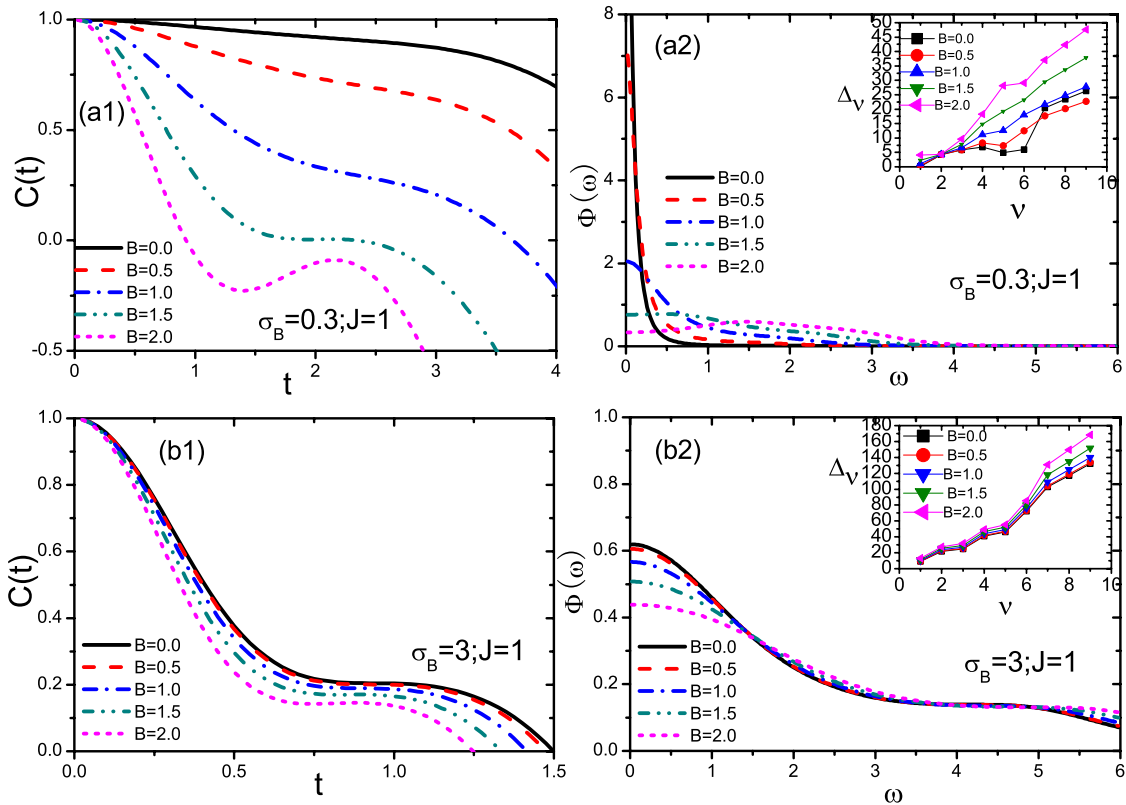


FIG. 7. (Color online) Autocorrelation functions and the corresponding spectral densities for $\sigma_B=0.3$ and $\sigma_B=3.0$. The system exhibits a crossover when σ_B is small [(a1) and (a2)]. However, when σ_B is large enough [(b1) and (b2)], only a disordered behavior is found.

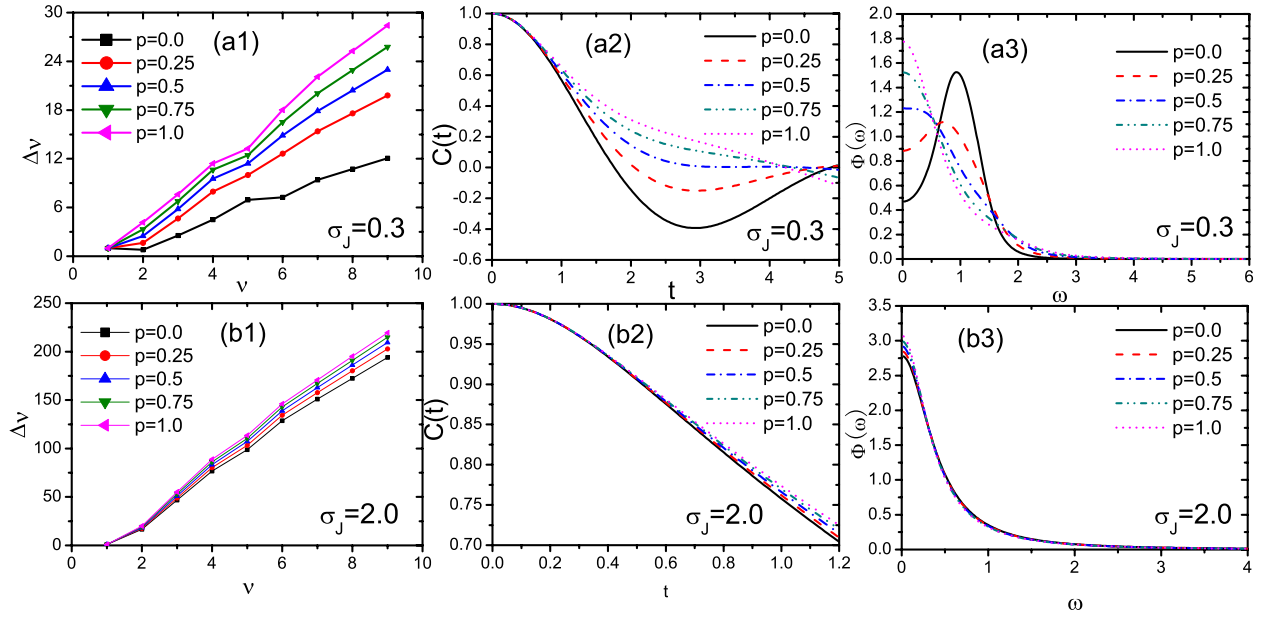


FIG. 8. (Color online) The recurrants, autocorrelation functions, and corresponding spectral densities for that the exchange couplings satisfy the double-Gaussian distribution and the external fields are constant. The results correspond to $J_1=1.0$ and $J_2=0.4$.

The system displays a disordered behavior which is a type of dynamical behavior between a collective-mode behavior and a central-peak one. The physical interpretation of the disordered behavior is that the large magnetic fields drive the spin orientation of the system to be disordered. By comparing the above results with that of 1D RTIM,¹⁵ we find that the central-peak behavior is more obvious.

IV. DOUBLE-GAUSSIAN DISTRIBUTION

Now, we consider a general distribution, namely, double-Gaussian distribution defined by

$$\rho(\beta_{i,j}) = p\rho_1(\beta_{i,j}) + (1-p)\rho_2(\beta_{i,j}), \quad (13)$$

where $\rho_1(\beta_{i,j})$ and $\rho_2(\beta_{i,j})$ with probabilities p and $1-p$, respectively, are Gaussian distributions [i.e., Eq. (12)], in which the mean value β of the $\rho_1(\beta_{i,j})$ is different from the $\rho_2(\beta_{i,j})$. This distribution can be used to describe a continuous distribution and a discrete one. Both bimodal and Gaussian distributions are the particular cases of the double-Gaussian distribution. Typically, when the standard deviation $\sigma_\beta \rightarrow 0$, the double-Gaussian distribution becomes a bimodal distribution. While $p=1$ or $p=0$, this distribution becomes Gaussian distribution.

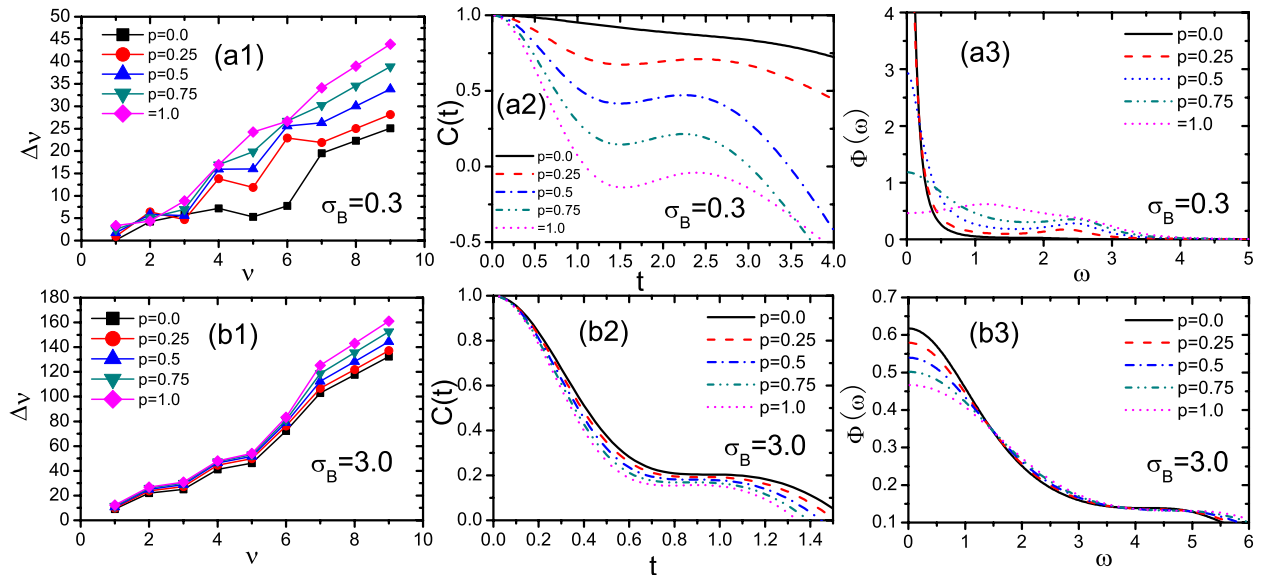


FIG. 9. (Color online) The recurrants, autocorrelation functions, and spectral densities for that the random-field satisfies the double-Gaussian distribution while $J_{ij,i'j'}=1$. The results correspond to $B_1=1.8$ and $B_2=0.2$.

In the following, we discuss the case that the exchange couplings $J_{ij,i'j'}$ satisfy the double-Gaussian distribution while the transverse fields $B_{i,j}$ are constants ($B_{i,j}=B=1$). Let the mean values of the exchange couplings in the distribution take $J_1=1.0$ and $J_2=0.4$. For the typical cases that the standard deviations σ_J take 0.3 and 2.0, the corresponding results of $C(t)$ and $\Phi(\omega)$ are shown in Fig. 8. It indicates that when $\sigma_J=0.3$, the system undergoes a crossover from a collective-mode behavior to a central-peak one as the concentration p increases. When σ_J is large enough ($\sigma_J=2.0$), the system only shows a central-peak behavior.

Consider another case that $B_{i,j}$ satisfy the double-Gaussian distribution while $J_{ij,i'j'}=J=1$. Let the mean values of the fields take the values $B_1=1.8$ and $B_2=0.2$. The recurrences, autocorrelation functions and spectral densities for both cases of $\sigma_B=0.3$ and 3.0 are shown in Fig. 9. We also can see that there is a crossover mentioned above when σ_B is small ($\sigma_B=0.3$). However, when $\sigma_B=3.0$ [see Fig. 9, (b2) and (b3)], the system only shows a most disordered state.

V. CONCLUSIONS

In this paper, we have investigated the dynamics of the 2D RTIM at high-temperature limit by recurrence relations

method. We have calculated the autocorrelation functions and corresponding spectral densities for the cases that the exchange couplings or the magnetic fields satisfy three typical distributions, respectively. It is found that the dynamics of the system is affected by the competition between the spin-spin interactions and the external fields, not by the disordered distribution. Generally speaking, when σ_J or σ_B is small, the system undergoes a crossover from central-peak behavior to a collective-mode behavior as J/B decrease. However, when the large σ_J or σ_B , the system exhibits a central-peak behavior or a disordered behavior, respectively.

ACKNOWLEDGMENTS

This work is supported by the National Natural Science foundation of China under Grant No. 10775088, the Shandong Natural Science foundation under Grant No. Y2006A05, and the Science foundation of Qufu Normal University. S.X.C. would like to acknowledge many fruitful discussions with Wen-Jun Chen, Sai Wang, and Sheng-Xin Liu.

*Corresponding author; kongxm@mail.qfnu.edu.cn

- ¹J. Kötztler, H. Neuhaus-Steinmetz, A. Froese, and D. Görlitz, *Phys. Rev. Lett.* **60**, 647 (1988); R. W. Youngblood, G. Aepli, J. D. Axe, and J. A. Griffin, *ibid.* **49**, 1724 (1982); J. M. R. Roldan, B. M. McCoy, and J. H. H. Perk, *Physica A* **136**, 255 (1986); M. Böhm and H. Leschke, *ibid.* **199**, 116 (1993).
- ²J. H. H. Perk, H. W. Capel, G. R. W. Quispel, and F. W. Nijhoff, *Physica A* **123**, 1 (1984); B. Boechat, R. R. dos Santos, and M. A. Continentino, *Phys. Rev. B* **49**, 6404 (1994); M. A. Continentino, B. Boechat, and R. R. dos Santos, *ibid.* **50**, 13528 (1994).
- ³B. M. McCoy, E. Barouch, and D. B. Abraham, *Phys. Rev. A* **4**, 2331 (1971).
- ⁴H. G. Vaidya and C. A. Tracy, *Phys. Lett. A* **68**, 378 (1978).
- ⁵B. M. McCoy, J. H. H. Perk, and R. E. Shrock, *Nucl. Phys. B* **220**, 269 (1983); G. Müller and R. E. Shrock, *Phys. Rev. B* **29**, 288 (1984).
- ⁶A. Sur, D. Jasnow, and I. J. Lowe, *Phys. Rev. B* **12**, 3845 (1975); U. Brandt and K. Jacoby, *Z. Phys. B* **25**, 181 (1976); H. W. Capel and J. H. H. Perk, *Physica A* **87**, 211 (1977).
- ⁷J. Florencio, Jr. and M. H. Lee, *Phys. Rev. B* **35**, 1835 (1987).
- ⁸A. R. Its, A. G. Izergin, V. E. Korepin, and N. A. Slavnov, *Phys. Rev. Lett.* **70**, 1704 (1993); J. Stolze, A. Nöppert, and G. Müller, *Phys. Rev. B* **52**, 4319 (1995).
- ⁹Th. Niemeijer, *Physica (Amsterdam)* **36**, 377 (1967).
- ¹⁰S. Katsura, T. Horiguchi, and M. Suzuki, *Physica (Amsterdam)* **46**, 67 (1970).
- ¹¹J. Florencio and F. C. Sá Barreto, *Phys. Rev. B* **60**, 9555 (1999).
- ¹²B. Boechat, C. Cordeiro, J. Florencio, F. C. Sá Barreto, and O. F. de Alcantara Bonfim, *Phys. Rev. B* **61**, 14327 (2000).
- ¹³Maria Eugenia Silva Nunes and J. Florencio, *Phys. Rev. B* **68**, 014406 (2003).
- ¹⁴M. E. S. Nunes, J. A. Plascak, and J. Florencio, *Physica A* **332**, 1 (2004).
- ¹⁵Z.-Q. Liu, X.-M. Kong, and X.-S. Chen, *Phys. Rev. B* **73**, 224412 (2006).
- ¹⁶Z.-B. Xu, X.-M. Kong, and Z.-Q. Liu, *Phys. Rev. B* **77**, 184414 (2008).
- ¹⁷X.-J. Yuan, X.-M. Kong, Z.-B. Xu, and Z.-Q. Liu, *Physica A* **389**, 242 (2010).
- ¹⁸L. Onsager, *Phys. Rev.* **65**, 117 (1944).
- ¹⁹J. Florencio, Jr., S. Sen, and Z.-X. Cai, *J. Low Temp. Phys.* **89**, 561 (1992).
- ²⁰S. Biswas, A. K. Chandra, and P. Sen, *Phys. Rev. E* **78**, 041119 (2008).
- ²¹M. H. Lee, *Phys. Rev. B* **26**, 2547 (1982); *Phys. Rev. Lett.* **49**, 1072 (1982); *J. Math. Phys.* **24**, 2512 (1983).
- ²²P. Grigolini, G. Grosso, G. Pastori Parravicini, and M. Sparpaglione, *Phys. Rev. B* **27**, 7342 (1983); M. Giordano, P. Grigolini, D. Leporini, and P. Marin, *Phys. Rev. A* **28**, 2474 (1983).
- ²³S. Sen, *Physica A* **222**, 195 (1995).
- ²⁴J. Stolze, V. S. Viswanath, and G. Müller, *Z. Phys. B: Condens. Matter* **89**, 45 (1992).
- ²⁵J. Florencio, O. F. de Alcantara Bonfim, and F. C. Sá Barreto, *Physica A* **235**, 523 (1997).
- ²⁶M. S. L. du Croo de Jongh and J. M. J. van Leeuwen, *Phys. Rev. B* **57**, 8494 (1998).
- ²⁷Z. Friedman, *Phys. Rev. B* **17**, 1429 (1978).